



## Measurement of the Top Quark Mass in the Dilepton Channel Using the Matrix Weighting Method at DØ

The DØ Collaboration  
URL <http://www-d0.fnal.gov>  
(Dated: August 13, 2007)

We present a preliminary measurement of the top quark mass based on 57 dilepton events in the  $ee$ ,  $e\mu$ , and  $\mu\mu$  channels from about  $1 \text{ fb}^{-1}$  of data collected by the DØ experiment during Run II of the Fermilab Tevatron collider. We measure  $m_t = 175.2 \pm 6.1(\text{stat}) \pm 3.4(\text{syst}) \text{ GeV}$  in good agreement with the world average top quark mass.

*Preliminary Result*

## I. INTRODUCTION

We present a measurement of the top quark mass based on about  $1 \text{ fb}^{-1}$  of data from  $p\bar{p}$ -collisions at  $\sqrt{s}=1.96 \text{ TeV}$  collected by the DØ experiment during Run II. This is an update of an earlier Run II measurement [1], and is similar to the measurement on Run I data [2].

The top quark mass is an important parameter in standard model predictions. Loops involving top quarks provide the dominant radiative corrections to the value of the  $W$  boson mass, for example. Another important correction to the  $W$  boson mass originates from loops involving the Higgs boson. Thus precise measurements of the  $W$  boson and top quark masses provide a constraint on the Higgs boson mass.

## II. THE DØ DETECTOR

The DØ detector is a typical multipurpose collider detector, that consists of central tracking, calorimeter, and muon detection systems.

The magnetic central-tracking system is comprised of a silicon microstrip tracker and a scintillating fiber tracker, both located within a 2 T superconducting solenoidal magnet [3]. Central and forward preshower detectors are located just outside of the coil and in front of the calorimeters. The liquid-argon/uranium calorimeter is divided into a central section covering pseudorapidity  $|\eta| \leq 1$  and two end calorimeters extending coverage to  $|\eta| \leq 4$  [4]. In addition to the preshower detectors, scintillators between the calorimeter cryostats provide sampling of developing showers at  $1.1 < |\eta| < 1.4$ . The muon system is located outside the calorimeter and consists of a layer of tracking detectors and scintillation trigger counters before 1.8 T toroids, followed by two similar layers outside the toroids. Tracking at  $|\eta| < 1$  relies on 10 cm wide drift tubes [4], while 1 cm mini-drift tubes are used at  $1 < |\eta| < 2$ .

The trigger and data acquisition systems are designed to accommodate the high luminosities of Run II. Based on information from tracking, calorimeter, and muon systems, the output of the first level of the trigger is used to limit the rate for accepted events to  $\approx 1.5 \text{ kHz}$ . At the next trigger stage, with more refined information, the rate is reduced further to  $\approx 800 \text{ Hz}$ . These first two levels of triggering rely mainly on hardware and firmware. The third and final level of the trigger, with access to all of the event information, uses software algorithms and a computing farm, and reduces the output rate to  $\approx 50 \text{ Hz}$ , which is written to tape.

## III. DATASET AND EVENT SELECTION

### A. Monte Carlo Samples

The  $t\bar{t}$  and diboson Monte Carlo samples used in this analysis are generated using PYTHIA [5] as the event generator. We also generate samples containing a  $Z$  boson and either light jets ( $Zjj$ ) or heavy flavor jets from gluon splitting ( $Zbb, Zcc$ ) using using Alpgen [6], using PYTHIA to shower the generated partons and following the MLM prescription [7] for matching the parton shower to the matrix element. All Monte Carlo samples use GEANT [8] to simulate the detector response. Weights have been applied to events to account for electron and muon identification efficiencies, the  $Z p_T$  spectra in Monte Carlo, and the efficiency to pass the DØ trigger system.

### B. Event Selection

The event selection in each channel is identical to those used for the cross section measurement [10]. The yields are given in Table I.

TABLE I: Expected and observed event yields.

source	$t\bar{t}$ (7 pb)	$WW, Z$	fake $e$ or $\mu$	total	obs.
$ee$	$9.5 \pm 1.5$	$2.8 \pm 0.4$	$0.2^{+0.2}_{-0.1}$	$12.5 \pm 1.8$	16
$e\mu$	$28.6^{+2.1}_{-2.4}$	$5.0 \pm 0.9$	$1.8 \pm 0.6$	$35.3^{+2.8}_{-3.8}$	32
$\mu\mu$	$5.8 \pm 0.5$	$3.2 \pm 0.4$	$0.4 \pm 0.2$	$9.4 \pm 0.7$	9

## IV. ANALYSIS TECHNIQUE

### A. Matrix Weighting

As done previously, we follow the ideas proposed by Dalitz and Goldstein [11] to reconstruct events from decays of top-antitop quark pairs with two charged leptons (either electrons or muons) and two or more jets in the final state.

We use only the two jets with the highest  $p_T$  in this analysis. We assign these two jets to the  $b$  and  $\bar{b}$  quarks from the decay of the  $t$  and  $\bar{t}$  quarks. If we assume a hypothesized value for the top quark mass we can determine the pairs of  $t$  and  $\bar{t}$  momenta that are consistent with the observed lepton and jet momenta, and missing  $p_T$ . We call a pair of top-antitop quark momenta that is consistent with the observed event a solution. We assign a weight to each solution, given by

$$w = f(x)f(\bar{x})p(E_\ell^*|m_t)p(E_{\bar{\ell}}^*|m_t) \quad (1)$$

where  $f(x)$  is the Parton Distribution Function (PDF) for the proton for the momentum fraction  $x$  carried by the initial quark, and  $f(\bar{x})$  is the corresponding value for the initial antiquark. The quantity  $p(E_\ell^*|m_t)$  is the probability for the hypothesized top quark mass  $m_t$  that the lepton  $\ell$  has the observed energy in the top quark rest frame [11].

There are two ways to assign the two jets to the  $b$  and  $\bar{b}$  quarks. For each assignment of observed momenta to the final state particles, the ambiguity of the neutrino momenta allows up to four solutions for each hypothesized value of the top quark mass. The likelihood for each value of the top quark mass  $m_t$  is then given by the sum of the weights over all the possible solutions:

$$W_0(m_t) = \sum_{\text{sol}} \sum_{\text{assign}} w_{ij} \quad (2)$$

In the mass analysis procedure described so far we implicitly assume that all momenta are measured perfectly. The weight  $W_0(m_t)$  therefore is zero if no exact solution is found. However, the probability to observe this event if the top quark mass has the value  $m_t$  does not have to be zero if no exact solution is found, because of the finite resolution of the momentum measurements. We account for this by repeating the weight calculation with input values for the electron, jet, and muon momenta that are drawn from distributions which match the known detector resolutions. We then average the weight curves obtained from  $N$  such variations:

$$W(m_t) = \frac{1}{N} \sum_{n=1}^N W_n(m_t) \quad (3)$$

We thus effectively integrate the weight  $W(m_t)$  over the final state parton momenta, weighted by the experimental resolutions. We refer to this procedure as resolution sampling. The main rationale for employing resolution sampling is that it increases the number of events for which we find solutions. In Monte Carlo events with an input top quark mass of 175 GeV, about 10% of the events have no solutions as measured. After sampling 500 times for each event the fraction of events without solutions drops to less than 1%.

For each event we use the value of the hypothesized top quark mass at which  $W(m_t)$  reaches its maximum as the estimator for the mass of the top quark. We call this mass value the peak mass. We cannot determine the top quark mass directly from the distribution of peak masses, because effects such as initial and final state radiation shift the most probable value of the peak mass distribution away from the actual top quark mass. We therefore generate the expected distributions of weight curve peaks for a range of top quark masses using Monte Carlo simulations. We call these distributions templates.

To extract the mass we use a binned maximum likelihood fit with the following definition for the likelihood:

$$\mathcal{L}(m_t) = \prod_{i=1}^{n_{bin}} \left[ \frac{n_s s_i(m_t) + n_b b_i}{n_s + n_i} \right]^{n_i} \quad (4)$$

Here  $n_i$  is the number of data events observed in bin  $i$ ,  $s_i(m_t)$  is the normalized signal template for bin  $i$  with top mass  $m_t$ ,  $b_i$  is the normalized background template, and  $n_s$  and  $n_b$  are the number of expected signal and background events taken from table I.

We finally fit a quadratic function to the  $-\log \mathcal{L}$ , including all values of  $-\log \mathcal{L}$  for top quark masses within  $\pm 20$  GeV of the mass for which  $-\log \mathcal{L}$  is smallest.

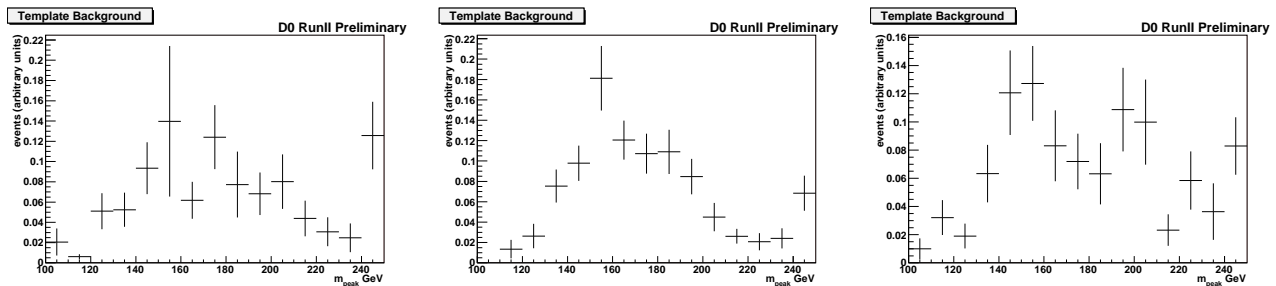


FIG. 1: Combined background templates for  $ee$ ,  $\mu\mu$ , and  $e\mu$

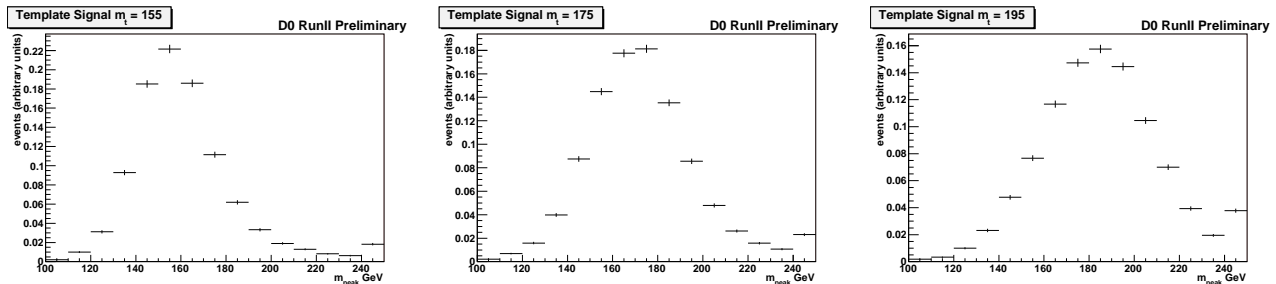


FIG. 2: Templates from Monte Carlo events from  $t\bar{t}$  decays to  $e\mu$  for  $m_t = 155$  GeV (left), 175 GeV (center), and 195 GeV (right).

## V. PERFORMANCE WITH $D\bar{O}$ MONTE CARLO EVENTS

### A. Calibration of the method

In order to demonstrate the performance of our method, we generate a large number of simulated experiments for several input top quark mass values. We refer to each of these experiments as an ensemble. We fit each of the ensembles to the templates as for collider data (see figures 1, 2). The distribution of measured top quark mass values from the ensemble fits gives an estimate of the parent distribution of our measurement.

We fix the number of events in an ensemble to the number of observed data events. Each event is randomly drawn from the signal or background Monte Carlo samples with a probability proportional to the number of events expected from each sample. Having chosen a sample to draw an event from, we choose a random event, and then accept or reject the event by comparing the event weight to a random number. We calculate the likelihood at each mass point according to equation 4. For convenience we fit the negative log of the likelihood with a second order polynomial. Finally, we combine the channels by adding together the negative log likelihoods for each channel.

Figure 3 shows distributions of the measured top quark mass, the statistical uncertainty obtained from the likelihood fit, and the pull for an input top quark mass of 175 GeV from ensemble tests. The results of ensemble tests for a range of input top quark masses are summarized in Figure 4. We have calibrated our result to remove any systematic bias in the measured top quark mass and in the statistical uncertainty, and the plots of mean errors and pull rms values reflect this calibration. For an ensemble, the pull is defined as the difference between the fitted mass ( $m_{fit}$ ) and the input top quark mass ( $m_{top}$ ) divided by the statistical uncertainty from the fit. For many ensembles the average pull should be zero and its rms should be one.

### B. Systematic Uncertainties

We use the ensemble test technique to study the size of the systematic uncertainties. We make systematic changes to the events in the ensembles, and fit them using the nominal templates. The change in the result gives the size of the systematic uncertainty.

- **Jet Energy Scale:** Since we compare the results from the collider data against simulated templates, the measurement will be systematically biased if the jet energies are calibrated differently in data and simulation. We

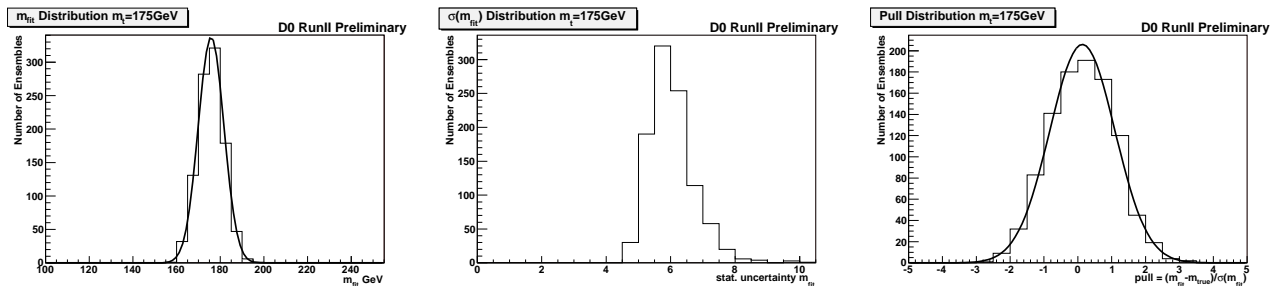


FIG. 3: Fitted mass distribution, error distribution, and pull distribution for 1000 ensembles with  $m_t = 175$  GeV for combination of channels.

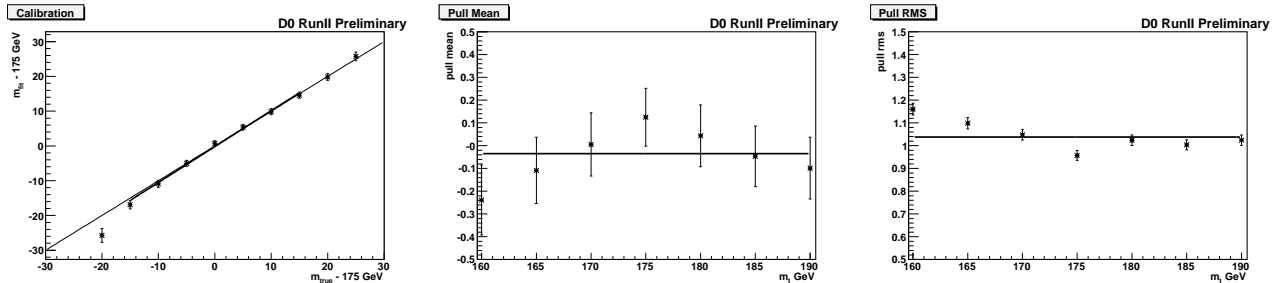


FIG. 4: Average fit mass, pull, and pull width versus input top quark mass for the ensemble tests for combination of channels.

vary all jet energies by  $\pm 1\sigma$  using errors parametrized in terms of the jet  $p_T$  and  $\eta$ . We then apply the selection cuts and perform ensemble tests using the two varied samples. We compare the results with the nominal sample and find the variation in  $m_t$  from this change to be  $\pm 2.4$  GeV.

- **b-jet Energy Scale:** The previous jet energy scale is derived from a sample composed primarily of light jets. Applying it to b-jets introduces an extra 1.5% error. This error introduces a shift in the top mass of  $\pm 1.7$  GeV.
- **Jet Energy Resolution:** The smearing applied to Monte Carlo jets is varied up and down within its uncertainties. This is found to shift the top mass by  $\pm 0.7$  GeV.
- **Background Fraction:** In order to estimate the effect of the uncertainty in the background estimation on the result, we increase and decrease the expected signal fraction from Table I in the ensembles by one sigma while keeping the nominal templates. This is useful as the method is not sensitive to shifts in the overall normalization, only to the relative contribution of signal and background. The systematic variation on the top mass is found to be 0.4 GeV.
- **Parton Distribution Function:** We estimate the effect of the uncertainty from the parton distribution functions by reweighting the Monte Carlo events in our ensembles up and down according to the 20 available error sets in the CTEQ6.1 PDF and then adding the systematic uncertainties obtained from each in quadrature. The uncertainty obtained in this way is 0.4 GeV.
- **Glucan Radiation:** To estimate the effect of gluon radiation we modify the ratio of 3 or more jet events to 2 jet events. A variation of 20% is chosen based on the difference between the ratio observed in data and the number expected from the Monte Carlo. Events with 3 jets are then reweighted to increase their contribution in the sample. The variation obtained in this way is 0.1 GeV.
- **Signal Modeling:** We estimate an uncertainty due to color recombination using a signal Monte Carlo sample generated using tune DW of the event generator PYTHIA, which includes a different model of color recombination. Using this different tune introduces a shift of 0.3 GeV, which we take as the systematic uncertainty.
- **Ensemble Calibration:** The mean of the fitted top mass fluctuates away from the nominal value by as much as 0.5 GeV. This value is taken as a systematic uncertainty.
- **Template Statistics:** The events used to form templates are split into four parts, ensemble tests are performed separately using each part, and the average of the variations is found to be 0.9 GeV.

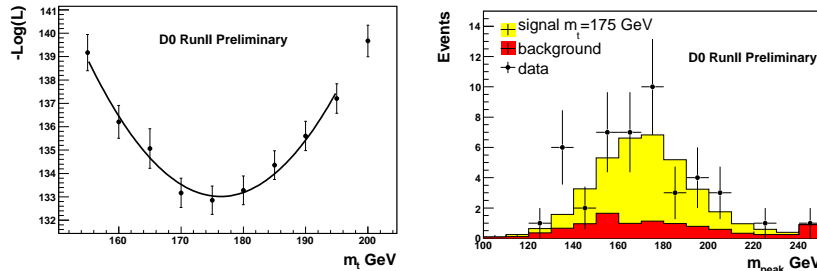


FIG. 5: Plots of  $-\ln L$  versus top quark mass (left) and comparison of peak masses in data and Monte Carlo (right).

## VI. RESULT

The fit results have to be corrected for the small offsets observed in the calibration (see Figure 4) and for the pull widths.

The calibrated result for the combination of the three channels (see figure 5), with systematics, is:

$$m_t = 175.2 \pm 6.1(stat) \pm 3.4(syst) \text{ GeV},$$

Table II summarizes the uncertainties. The world average top quark mass measurement based on Run I and Run II data collected by CDF and DØ is  $m_t = 170.9 \pm 1.8 \text{ GeV}$  [14]. Our result is consistent with the world average value.

TABLE II: Summary of uncertainties.

source	uncertainty
statistical uncertainty	6.1 GeV
systematic	3.4 GeV
jet energy scale	2.4 GeV
b-jet energy scale	1.7 GeV
jet energy resolution	0.7 GeV
background fraction	0.4 GeV
background shape	1.0 GeV
parton distribution functions	0.4 GeV
signal modeling	0.3 GeV
gluon radiation	0.1 GeV
ensemble calibration	0.5 GeV
template statistics	0.9 GeV
total error	7.0 GeV

- 
- [1] DØ note 5200, “Measurement of the Top Quark Mass in the  $e\mu$  Channel Using the Matrix Weighting Method at DØ”, July 2006.
- [2] DØ Collaboration, Phys. Rev. Letters 80, 2063 (1998); Phys. Rev. D 60, 052001 (1999).
- [3] DØ Collaboration, V. Abazov *et al.*, “The Upgraded DØ Detector”, submitted to Nucl. Instrum. Methods Phys. Res. A, and T. LeCompte and H.T. Diehl, Ann. Rev. Nucl. Part. Sci. **50**, 71 (2000).
- [4] DØ Collaboration, S. Abachi *et al.*, Nucl. Instrum. Methods Phys. Res. A **338**, 185 (1994).
- [5] T. Sjöstrand *et al.*, Computer Physics Commun. 135 (2001) 238.
- [6] M.L. Mangano, M. Moretti, F. Piccinini, R. Pittau, A. Polosa, JHEP 0307:001,2003, hep-ph/0206293.
- [7] S. Hoche, F. Krauss, N. Lavesson, L. Lonnblad, M. Mangano, A. Schaliche and S. Schumann, “Matching parton showers and matrix elements”, arXiv:hep-ph/0602031. M.L. Mangano, M. Moretti, R. Pittau, Nucl.Phys.B632:343-362,2002; hep-ph/0108069; F. Caravaglios, M. L. Mangano, M. Moretti, R. Pittau, Nucl.Phys.B539:215-232,1999; hep-ph/9807570.
- [8] S. Agostinelli *et al.*, Nuclear Instruments and Methods in Physics Research A506, 250 (2003).
- [9] DØ note 4914, “Shifting, Smearing, and Removing Simulated Jets”, November 2005.
- [10] DØ note 5371, “Measurement of the  $t\bar{t}$  Production cross section at  $\sqrt{s} = 1.96 \text{ TeV}$  in Dilepton Final States using  $1fb^{-1}$ ”, March 2007.

- [11] R.H. Dalitz and G.R. Goldstein, Phys Rev. D 45, 1531 (1992).
- [12] K. Kondo, J. Phys. Soc. Jpn. 57, 4126 (1988); 60, 836 (1991).
- [13] DØ note 4874-CONF “Top Quark Mass Measurement with the Matrix Element Method in the Lepton+Jets Final State at DØ Run II”, July 2005.
- [14] The CDF and DØ Collaborations, the Tevatron Electroweak Working Group, “Combination of CDF and DØ Results on the Top-Quark Mass”, hep-ex/0703034.